This is the accepted manuscript of the article, which has been published in *Journal of Virological Methods*. 2018, 255, 29-37. https://doi.org/10.1016/j.jviromet.2018.02.001

New Coxsackievirus 2A^{pro} and 3C^{pro} protease antibodies for virus detection and discovery of pathogenic mechanisms

Olli H. Laitinen[a], Emma Svedin[a], Sebastian Kapell[a], Minna M. Hankaniemi[b,c], Pär G. Larsson[a], Erna Domsgen[a], Virginia M. Stone[a], Juha A. E. Määttä[b,c], Heikki Hyöty[b,c], Vesa P. Hytönen[b,c], Malin Flodström-Tullberg[a,b]

[a]The Center for Infectious Medicine, Department of Medicine HS, Karolinska Institutet, Karolinska University Hospital, Stockholm, 141 86, Sweden.

[b] Faculty of Medicine and Life Sciences, University of Tampere, Tampere, 33520, Finland.

[c] Fimlab Laboratories, 33520 Tampere, Finland

Corresponding Author: Dr. Malin Flodström-Tullberg, The Center for Infectious Medicine, Department of Medicine HS, Karolinska Institutet, Karolinska University Hospital, Stockholm, 141 86, Sweden. malin.flodstrom-tullberg@ki.se

+46 76 947 4569

Short running title: Characterization of novel pan-Coxsackievirus antibodies

Word Count Abstract: 198

Word Count Main Text: 4457

ABSTRACT

Enteroviruses (EVs), such as the Coxsackie B-viruses (CVBs), are common human pathogens, which can cause severe disease including meningitis, myocarditis and neonatal sepsis. EVs encode two proteases ($2A^{pro}$ and $3C^{pro}$), which perform the proteolytic cleavage of the CVB polyprotein and also cleave host cell proteins to facilitate viral replication. The $2A^{pro}$ cause direct damage to the infected heart and tools to investigate $2A^{pro}$ and $3C^{pro}$ expression may contribute new knowledge on virus-induced pathologies. Here, we developed new antibodies to CVB-encoded $2A^{pro}$ and $3C^{pro}$; Two monoclonal $2A^{pro}$ antibodies and one $3C^{pro}$ antibody were produced. Using cells infected with selected viruses belonging to the EV A, B and C species and immunocytochemistry, we demonstrate that the $3C^{pro}$ antibody detects all of the EV species B (EV-B) viruses tested and that the $2A^{pro}$ antibody detects all EV-B viruses apart from Echovirus 9. We furthermore show that the new antibodies work in Western blotting, immunocyto- and immunohistochemistry, and flow cytometry to detect CVBs. Confocal microscopy demonstrated the expression kinetics and revealed a preferential cytosolic localization of the proteases in CVB3 infected cells. In summary, the new antibodies detect proteases that belong to EV species B in cells and tissue using multiple applications.

Key Words: Enterovirus; Coxsackievirus; Protease 2A; Protease 3C; Monoclonal antibodies

Abbreviations: $2A^{pro}$, Enteroviral protease 2A; $3C^{pro}$, Enteroviral protease 3C; EV, Enterovirus; CVA Coxsackievirus A; CVB Coxsackievirus B; RT-PCR, Real Time

Polymerase Chain Reaction; VP, Viral Protein; IHC, Immunohistochemistry; PFU, plaque forming unit; ICC, Immunocytochemistry; IMAC, Immobilized metal affinity chromatography

1. INTRODUCTION

Enteroviruses (EVs) are important human pathogens and they are the most common infectious viruses in humans, particularly in young children. EVs and especially the Coxsackievirus B (CVB) group have been associated with many diseases. These include acute illnesses such as severe infections in neonates, sepsis, meningitis, myocarditis, human foot-and-mouth disease and pancreatitis (Calderón et al., 2016; Gaaloul et al., 2014; Orbach et al., 2016; Persichino et al., 2016). In addition, EVs have been connected to chronic diseases such as type 1 diabetes and dilated cardiomyopathy (Gaaloul et al., 2014; Laitinen et al., 2014; N'Guyen et al., 2016; Oikarinen et al., 2014; Yeung et al., 2011).

The EV genome consists of a single positive stranded RNA molecule, with one open reading frame encoding the viral polyprotein. This polyprotein contains two viral proteases, $2A^{pro}$ and $3C^{pro}$, which perform the proteolytic cleavage of the polyprotein into the structural capsid proteins VP1-4 and nonstructural proteins required for virus replication. Further to this, the proteases also cleave host cell proteins in order to facilitate the propagation of the virus and to evade host cellular immune responses (Feng et al., 2014; Laitinen et al., 2016; Lamphear et al., 1993; Lei et al., 2013; Lind et al., 2016, 2014, 2013; Mukherjee et al., 2011; Weidman et al., 2001), which may also contribute to pathology. Indeed, the cleavage of cardiac specific proteins by the viral protease $2A^{pro}$ has been shown to contribute to CVB-induced myocarditis (Badorff et al., 2000; Barnabei et al., 2015; Lim et al., 2013; Luo et al., 2010; Massilamany et al., 2014; Wong et al., 2012). Given that the predicted substrate sequences for the proteases are present in numerous host proteins (Laitinen et al., 2016), it is likely that cleavage

of other human host proteins contributes to the damage in other organs during CVB infection.

To better understand the associations between EVs and various diseases and the potential mechanisms through which these viruses cause pathology, **appropriate** molecular tools are essential. Currently, available methods for detecting EVs in both clinical and research laboratories are mainly founded on nucleic acid recognition based methodologies (RT-PCR, hybridization and next generation sequencing) (Ettischer-Schmid et al., 2016; Kramná et al., 2015; Laiho et al., 2016; Maccari et al., 2016; Yousef et al., 1987), but antigen based immunoassays (Li et al., 2011; Zhang et al., 2016) have also been developed to detect virus-specific antibodies in serum samples. Moreover, mass spectrometry has been utilized to directly detect viral proteins in experimental and patient samples (Calderaro et al., 2014; Laiho et al., 2016). In clinical laboratories current trends focus predominantly on PCR-based techniques (Luoto et al., 2016), whereas antibody based approaches are widely used in academic research.

One of the most frequently used antibodies in EV detection is the monoclonal antibody clone 5-D8/1 (Maccari et al., 2016; Yousef et al., 1987), which recognizes an N-terminal epitope of the VP1 capsid protein (Samuelson et al., 1995) in a large spectrum of EV species A and B serotypes (Laiho et al., 2015; Miao et al., 2009). Currently, antibodies specifically targeting CVB encoded proteases are rare and to our knowledge, none are commercially available highlighting the need for their development.

In the present study we introduce novel monoclonal rat antibodies raised against the CVB proteases $2A^{pro}$ and $3C^{pro}$, and describe several applications by which they successfully detect EVs, including Western blotting, immunocyto- and

immunohistochemistry and flow cytometry. Using these reagents we also provide additional insight into the kinetics of protease expression and cellular localization during acute infection in cultured cells.

2. MATERIALS AND METHODS

2.1. Cloning and production of $2A^{pro}$ and $3C^{pro}$

CVB3 Nancy (UniProtKB/Swiss-Prot: P03313.4) polyprotein sequence was used as a template to construct recombinant His-tagged $2A^{pro}$ and $3C^{pro}$ proteases. Artificial genes encoding the proteases were ordered from Life Technologies (Germany) and were cloned into the pBVboostFGII expression vector as described in (Heikura et al., 2012; Laitinen et al., 2005). Proteases were expressed in *E. coli*, strain BL21-AI (Life Technologies), and then purified with immobilized metal affinity chromatography (IMAC) using the ÄKTA P-100 liquid chromatography system and HisTrap FF crude IMAC columns (GE Healthcare Bio-Science AB).

2.2. Generation of hybridoma and production of antibodies

Monoclonal antibodies against CVB3 (Nancy) $2A^{pro}$ and $3C^{pro}$ proteases were produced through the immunization of Wistar rats with the purified proteases (GenScript, Hong Kong). Hybridomas were generated by electrofusion and the positive clones were positively selected for the detection of the proteases and negatively selected for their recognition of the His-tag by ELISA (Genscript). After initial Western blotting using CVB3 infected HeLa cell lysates (see below) and immunohistochemistry (IHC) screening using pancreas tissue from CVB infected mice (see below), two $2A^{pro}$ recognizing antibody clones (denoted 2A-1 and 2A-2) and one $3C^{pro}$ clone (denoted

3C) were selected for antibody production and the resulting antibodies were used in the present study.

2.3. Cell lines, viruses and cell microarray

HeLa cells, grown in standard RPMI 1640 medium supplemented with 10% inactivated fetal bovine serum (FBS) and 2 mM L-glutamine at 37 °C and 5% CO_2, were utilized for virus infections (Lind et al., 2016). Cells were passaged the day before infection. The generation of the cell microarray encompassing green monkey kidney cells (GMK and Vero), carcinomic human alveolar basal epithelial cells (A549), human rhabdomyosarcoma muscle cells (RD) and carcinomic human cervix epithelial cells (HeLa) infected with a selection of human **viruses has been reported** (Laiho et al., 2015). A list of the viruses used in this study, is presented in Supplementary Table 1.

2.4. Western blot

HeLa cells were infected with one of the six CVB serotypes (MOI 20) and the infections were terminated at the indicated time points. Mock infected cells served as controls. Proteins were isolated, separated by SDS-PAGE and detected using Western blot, as described in (Lind et al., 2013). The recombinant proteases were used as positive controls. Primary antibodies used were as follows: 2A-1 diluted 1:2000 from a 100 µg/ml stock and 3C diluted 1:2000 from a 180 µg/ml stock, VP1 (1:500, clone 5-D8/1, Dako Cytomation, Denmark) and anti-actin (1:30,000, MP Biomedicals, Aurora, Ohio, USA). The secondary antibodies utilized were HRP conjugated goat-anti mouse for the

VP1 and actin antibodies (Bio-Rad, 1:1000 dilution) and goat anti-rat for 2A and 3C antibodies (Bio-Rad, 1:10,000).

2.5. Intracellular flow cytometry

HeLa cells were infected for 6h with the indicated CVBs (MOI 20), after which the cells were fixed with 1% paraformaldehyde at room temperature. Mock infected cells served as controls. Permeabilization and intracellular staining were performed in Perm/Wash (BD) using anti-VP1 antibody (clone 5-D8/1, Dako, diluted 1:50) and/or the primary rat 2A-2 or 3C antibodies diluted 1:250 or 1:50 from 100 µg/ml stocks respectively. The primary antibodies were detected using a goat anti-mouse Alexa Fluor 647- or Alexa Fluor 488-conjugated secondary antibodies (Invitrogen; VP1), or a phycoerythrin (PE) labeled goat anti-rat IgG antibody (Invitrogen; 2A-2 and 3C). VP1 and protease positive cells were detected with a BD Accuri™ C6 and BD Fortessa. Samples were analyzed using FlowJo software (Tree Star).

2.6. Animals

C57BL6 and non-obese diabetic (NOD) mice were bred and housed in a specific-pathogen-free environment at Karolinska Institutet, Stockholm, Sweden. Animals were infected with 10^3-10^8 PFU CVB1, -3, -4 or -5 administered in 200 µl RPMI 1640 via the intraperitoneal route. Untreated mice, or those mock-infected with RPMI 1640 alone served as controls. Systemic viral spread was confirmed by viremia measurements using plaque assay or RT-PCR on days 3-5 post infection (data not shown), as previously described (Larsson et al., 2015). All animal experiments were

approved by a local ethics committee and conducted in accordance with the NIH principles of laboratory animal care and the Swedish law.

2.7. Immunocyto- and immunohistochemistry

Pancreas tissue, harvested from CVB infected mice between day 3 and 5 post infection, were fixed in 4% formaldehyde in PBS for 24 h. Negative control samples were collected from uninfected mice. After dehydration and paraffin embedding, the formalin-fixed paraffin embedded (FFPE) tissues were cut in 0.5 µm thick sections and heat-fixed to Superfrost® Plus microscope slides (Thermo Scientific, Germany).

Prior to immunocytochemical (ICC, cell microarray) and IHC (tissue sections) staining, antigen retrieval was performed by boiling samples for 2 x 2.5 min in buffer containing 10 mM citrate pH 6 (2A-2) or 10 mM Tris and 1mM EDTA pH 9 (3C and VP1-bio; see below). Comprehensive antibody titrations were performed and optimal dilutions were determined to be 1:4000 for the 2A-2 antibody and 1:100 for the 3C antibody (both from 100 µg/ml antibody stocks). Detection was performed with a biotinylated goat anti-rat IgG antibody (Vector Laboratories, USA). Staining with the secondary antibody alone showed no positivity (data not shown). To confirm the presence of virus, sequential tissue sections were probed with a biotinylated VP1 antibody (clone 5-D8/1, Dako Cytomation, Denmark). As this antibody is of murine origin, it was biotinylated (Capra Science, Sweden) before use (hence denoted VP1-bio). The VP1-bio antibody was used at a 1:100 dilution (70 µg/ml stock), and due to the biotinylation, no secondary antibody was required. Staining in ICC and IHC was visualized using horseradish peroxidase-coupled streptavidin (ABC kit, Vector labs) and DAB substrate (Vector labs).

2.8. Confocal microscopy

HeLa-cells grown on glass coverslips were infected with CVB3 (Nancy, MOI 20) for 2, 4 or 6 h. The cells were fixed with 4% PFA and permeabilized with 0.2% Triton-X100. Cells were stained with either 2A-2 (1:100) or 3C (1:100) followed by an Alexa-fluor 488-conjugated secondary goat anti-rat IgG antibody (1:200; Thermo Fisher Scientific). Nuclear lamina was stained using a polyclonal antibody to Lamin B1 (ab16048, Abcam, 1:500) and the secondary antibody Alexa-fluor 568-**conjugated** goat anti-rabbit IgG (A11011, Life Technologies, 1:250). Nuclei were visualized with DAPI 285 nM (Sigma). Cells were covered with ProLong Diamond antifade reagent (Molecular Probes) and the staining was analyzed by confocal microscopy (Nikon A1R). Alexa 488 was excited with a 488 nm laser and fluorescence was collected with a 500-550 nm band-pass filter. Alexa 568 was excited with a 561 nm laser and the fluorescence was collected with a 570-620 nm band-pass filter. DAPI was excited with 405 nm laser and fluorescence was collected with a 425-475 band-pass filter. The image size was adjusted to 1.024 x 1.024 pixels and 0.15 µm thick Z-stack slices were imaged with averaging of two images. The pinhole was set to 1.2 Airy unit.

3. RESULTS

3.1. Protease antibodies detect CVB1-6 infections by Western blot

Two monoclonal rat antibodies against CVB3 (Nancy) $2A^{pro}$ (here denoted 2A-1 and 2A-2) and one antibody against CVB3 (Nancy) $3C^{pro}$ were produced, as described in materials and methods. Western blot analysis of cell lysates prepared from CVB3 infected HeLa cells revealed that all three antibodies detected protein bands with the expected $2A^{pro}$ and $3C^{pro}$ molecular weights (data not shown). The 2A-1 and 3C antibodies were tested for their ability to detect recombinant $2A^{pro}$ and $3C^{pro}$. 2A-1 detected $2A^{pro}$ but not $3C^{pro}$, and the 3C antibody only detected $3C^{pro}$ (Figure 1A and B). A time course CVB infection study in HeLa cells revealed the appearance of $2A^{pro}$ in the cell lysate at 3 h post infection (Figure 1 C). The highest $2A^{pro}$ level was observed around 5 h post infection, after which the expression declined. In comparison, $3C^{pro}$ was initially detected at four hours post infection and was then present at a fairly constant level during the 9 h time course.

To investigate if the newly developed antibodies detect proteases of heterotypic, but closely related EVs, and to compare the antibodies with the commonly used anti-VP1 antibody clone 5-D8/1, further Western blot analyses were performed. HeLa cells were infected with either of the six CVB serotypes and cell lysates were harvested at 6 h post infection and analyzed with the different antibodies. The 2A-1 and 3C antibodies recognized bands with the expected size of $2A^{pro}$ and $3C^{pro}$, respectively, in cell lysates from all six CVB serotypes (Figure 1 D). The VP1 antibody, as expected, detected all

six serotypes however, of note, the recognition of CVB6 was weaker than the other serotypes, an observation which we have also previously documented (Saarinen et al., 2018). Contrastingly, both protease antibodies demonstrated a robust detection of CVB6.

3.2. EV serotype B (EV-B) species are recognized by the protease antibodies in immunocytochemistry

Given the ability of the protease antibodies to recognize viral proteins in lysates from CVB infected cells by Western blot, we next set out to determine if the antibodies could also detect viral proteins with ICC. To this end, an array of fixed and paraffin embedded human cell lines infected with various EVs was used (Table 1 and (Laiho et al., 2015)). The array also provides a method to determine the breadth of EVs that the antibodies can recognize. The 2A-1 and -2, 3C and VP1 antibodies were used to stain the cell array. However, pilot studies suggested that the 2A-1 antibody did not detect virus positive cells in formalin fixed tissue (data not shown) and therefore it was not used in these studies. 2A-2 detected cells infected with all six different CVB serotypes, Echovirus 4, 6, 11, 30 and CVA9, but it did not recognize any EV-A serotypes, poliovirus nor the human parechovirus 1 (Table 1). Positivity was also seen with the 3C antibody in cells infected with all six CVBs, Echovirus 3, 4, 6, 9, 11, 30 and CVA9. However, 2A-2 did not detect EV-A serotypes and poliovirus (Table 1). When compared to the commonly used VP1 antibody (DAKO, clone 5-D8/1), the 2A-2 and 3C antibodies demonstrated a higher level of selectivity in their recognition of viruses as they only detected EV-B serotypes, whereas the VP1 antibody detected many EV-A viruses. Uninfected cells and infected cells incubated with secondary antibody alone acted as negative controls and showed no positive staining (data not shown).

3.3. Protease antibodies detect CVBs in CVB infected mouse pancreas

To fully study the mechanisms behind virus-instigated pathologies, access to a comprehensive range of antibodies capable of detecting virus proteins in tissue samples from patients and in experimental disease models is highly advantageous. Mouse models have been widely utilized to study the pathogenesis of CVB-induced diseases. In contrast to many other EVs, CVBs are capable of infecting mice at any age and they also have a similar tissue tropism to that seen in humans, including the pancreas and heart. As such, mice have therefore become useful models for studies on myocarditis, pancreatitis and Type 1 diabetes (reviewed in (Fairweather et al., 2012; Jaïdane et al., 2009)).

In order to examine whether the protease antibodies are capable of detecting CVB proteases in tissue samples, we utilized pancreas tissue collected at different time points post infection from mice infected with CVB3 (homotypic detection) and CVB1, -4 and -5 (heterotypic detection). FFPE pancreas sections were stained with 2A-2, 3C or VP1-bio antibodies. CVBs typically infect the exocrine pancreas tissue in mice (Flodström et al., 2002; Jaïdane et al., 2010) and all of the antibodies successfully stained the exocrine tissue in CVB infected animals (CVB3 and -5 infected animals, Figure 2; CVB1 and -4, data not shown). As expected (Flodström et al., 2002; Jaïdane et al., 2010), none of the antibodies detected viral proteins in the pancreatic islets of these infected mice (Figure 2 and data not shown). Furthermore, there was an absence of non-specific staining in the pancreas of uninfected control mice (Fig 2 A, C, E and G).

3.4. CVB infected cells are detected by flow cytometry using the protease antibodies

In flow cytometry, single cells can be counted and sorted with simultaneous qualitative and quantitative analysis of multiple parameters. As such, antibodies targeting proteins of interest are important tools in classical flow cytometry-based analyses and can be either directly conjugated with a fluorescent label or used in combination with a labeled secondary antibody. Flow cytometry has been used in EV research to, for example, identify infected cells (Hühn et al., 2007), assess the expression kinetics of VP1, to study the efficacy of cytokines in regulating cellular permissiveness to infection (Lind et al., 2016), and to study changes in the host immune system during infection (Lincez et al., 2015).

To evaluate the usefulness of the $2A^{pro}$ and $3C^{pro}$ antibodies in flow cytometry, HeLa cells were infected with CVB3 for 6 h. The cells were then fixed, permeabilized and stained with antibodies prior to flow cytometry analysis. The 2A-2 and 3C antibodies, as well as the VP1 clone 5-D8/1 antibody, positively stained infected cells and were detected by flow cytometry (Figure 3 A).

Next, double staining was performed in cells infected with CVB3 by combining one of the protease antibodies with the VP1 antibody. Flow cytometry analysis revealed double positive cells with the majority of VP1 positive cells being co-stained by the 2A and 3C antibodies, respectively (Figure 3 B and C).

3.5. $2A^{pro}$ and $3C^{pro}$ mainly localize in the cytoplasm of acutely infected cells

Advanced microscopy methods, such as confocal microscopy, allow studies examining the cellular location of specific proteins. Here, confocal microscopy was employed to examine the suitability of the protease antibodies in visualizing the proteases during CVB3 infection. HeLa cells were infected by CVB3 for 2, 4 or 6 h and stained with the protease antibodies, followed by examination of their intracellular localization over time. The protease antibodies stained infected cells but not uninfected control cells. Assessment of the expression patterns revealed that $2A^{pro}$ staining was most intense four hours after infection (Figure 4 A and B), whereas the $3C^{pro}$ staining was strongest at six hours post infection (Figure 4 D and E). A strong staining was seen in the cytosol with both protease antibodies, whereas nuclear expression was weak in both cases (Figure 4 C and F).

4. DISCUSSION

In the present study we introduce three new monoclonal rat antibodies that detect $2A^{pro}$ and $3C^{pro}$ proteases in all of the known six CVB serotypes, as well as proteases from several other species B EVs. EVs, such as the common CVBs, cause pathologies and in this process, the functional proteins (e.g. the proteases), rather than the viral genome or the capsid proteins may elicit most of the damage (Badorff et al., 2000; Barnabei et al., 2015; Lim et al., 2013; Luo et al., 2010; Massilamany et al., 2014; Wong et al., 2012). In this respect, the $2A^{pro}$ and $3C^{pro}$ proteases are a pernicious twosome, as they are responsible for shutting down many vital cellular functions (Laitinen et al., 2016; Lamphear et al., 1993; Weidman et al., 2001), inhibiting the host's immune response to the virus (Feng et al., 2014; Lei et al., 2013; Lind et al., 2016, 2014, 2013; Mukherjee et al., 2011) and causing pathogenic changes in certain cell types and tissues (Badorff et al., 2000; Barnabei et al., 2015; Lim et al., 2013; Luo et al., 2010; Massilamany et al., 2014; Wong et al., 2012). There has been a lack of tools to study $2A^{pro}$ and $3C^{pro}$ and methods to examine their presence and involvement in cellular processes are likely to further enhance our understanding of the mechanisms through which the CVBs cause pathology. Such information may open possibilities for the development of therapeutics to use in viral diseases.

One of the strengths of the new protease antibodies presented here is their usefulness in numerous applications including Western blot, flow cytometry, ICC and IHC. A single monoclonal antibody detecting $3C^{pro}$ (3C) was compatible with all of the methods tested. In contrast, the two $2A^{pro}$ antibodies showed differences in their

usefulness in the various methodologies. While both the 2A-1 and the 2A-2 antibodies were functional in Western blot, only 2A-2 successfully detected virus in formalin fixed pancreas from infected mice. Moreover, the 2A-2 antibody also worked in ICC, confocal microscopy and intracellular flow cytometry.

Besides their suitability to detect the homotypic virus, CVB3, in various techniques, the protease antibodies recognized the other five CVB serotypes. Through IHC analysis of cells infected with a selection of other EV species, we found that the antibodies were capable of detecting some echoviruses and CVA9. We also compared the ability of the $2A^{pro}$ and $3C^{pro}$ antibodies to detect EVs in ICC with the VP1 antibody clone 5-D8/1, which detects EV species A and some EV species C viruses (namely poliovirus) (Laiho et al., 2015). Our results suggest that the protease antibodies are more EV species-specific than the VP1 antibody. This notion is also supported by phylogenetic analyses of VP1, $2A^{pro}$ and $3C^{pro}$ (Supplementary Figures 1-3), in which the proteases sequences recognized by 2A-2 and 3C are clustered tightly, whereas the VP1 sequence detected by 5-D8/1 is distributed over several clades. The antigen binding site of the VP1 antibody produced by clone 5-D8/1 has been shown to locate close to the N-terminus of VP1 (Samuelson et al., 1995), and is known to be well conserved between EVs (Maccari et al., 2016), thereby explaining its broader recognition profile.

EV-Bs, including the CVBs, are prone to recombination and both inter- and intra-serotypic recombinations have been described (Oberste et al., 2004a, 2004b). Such events could alter the amino acid sequences of $2A^{pro}$ and $3C^{pro}$ and thereby potentially also modulate the ability of the new antibodies which were raised to the prototype virus CVB3 Nancy to detect more recent virus isolates. Additional studies are required to investigate the efficacy of the new antibodies to detect a

larger number of such recent isolates. We however find that the 2A ^{pro} and 3C ^{pro} antibodies bind to viruses of all six CVB serotypes and other EV-Bs, some of which have been isolated more recently than CVB3 Nancy, including a CVB1 isolate from 1998, and echo3 and CVA9 isolated in 1998 and 2005, respectively (Supplementary Table 1). Moreover, a comparison of the 2A^{pro} and 3C^{pro} amino acid sequences from different EV-Bs showed a high level of conservation (Laitinen et al., 2016). Thus, it is likely that the new antibodies will be able to detect a broad range of more recent and currently circulating CVBs.

In this study, the antibodies produced were made by immunizing rats with recombinant 2A^{pro} and 3C^{pro}. During infection, the EV genome is translated into a polyprotein, which is cleaved into the structural and nonstructural proteins by 2A^{pro} and 3C^{pro}. Occasionally, our Western blot analyses of CVB infected HeLa cell lysates revealed staining of a few bands with a higher molecular weight than those expected for 2A^{pro} and 3C^{pro}. These bands correlate with the estimated sizes of parts of the viral polyprotein that have not been fully processed (data not shown). Hence, it is likely that the antibodies also detect unprocessed 2A^{pro} and 3C^{pro}. Such bands were not found in the cell lysates of uninfected cells. These bands were also not observed when the antibodies were used to detect recombinant 2A^{pro} and 3C^{pro}, except in the case of the dimer band observed for 3C^{pro} (Figure 1B). The dimeric forms of these proteases have also been observed in previous studies as reviewed in (Laitinen et al., 2016).

The VP1 antibody clone 5-D8/1 is an excellent tool for the detection of a broad range of EVs. In some applications and/or studies, it may be beneficial to use antibodies that recognize a narrower span of EV groups or even single EV serotypes (Ettischer-Schmid et al., 2016; Man-Li et al., 2012; Miao et al., 2009; Yagi et al., 1992). With regards to

this, it is interesting to note that the 3C antibody detected all of the EV-B viruses examined, and similarly, the 2A-2 antibody detected all except for Echo9, thereby indicating that that both antibodies, and particularly 3C, could constitute excellent EV-B detection tools. Additional screening with these protease antibodies of all known EV-B viruses and other viruses outside the EV-B serotypes could be performed to guarantee that recognition is limited to EV-B viruses. Such screening should also be performed to verify the specificity of the antibodies in detecting EV-B viruses in other applications including ELISA, IHC, flow cytometry and Western blot. If further validation confirms that these protease antibodies are specific for EV species B viruses, then they could be utilized to complement current technologies employed in the identification of EVs in research and clinical samples (Kramná et al., 2015; Laiho et al., 2016; Luoto et al., 2016).

Many experimental EV disease models have been developed in the mouse (Fairweather et al., 2012; Jaïdane et al., 2009). For IHC studies in mouse tissues, primary monoclonal antibodies of rat origin provide an advantage over those generated in mice. If primary mouse antibodies are not directly conjugated, their detection requires the use of a secondary antibody directed to mouse immunoglobulins and this secondary antibody will inevitably bind to endogenous mouse immunoglobulins present in the tissue providing high background staining. This is, for example, a challenge faced with the VP1 antibody (clone 5-D8/1), which is of mouse origin. In the present study, the VP1 antibody was directly biotinylated to omit the need for a secondary antibody, thereby rendering it compatible for staining mouse tissue. The 2A and 3C antibodies described were generated in rat, which bypasses the need for additional modification before use in mouse tissue and further to this, the antibodies should also be suitable for use in human tissue samples.

In the end of our studies, we also addressed the usefulness of the protease antibodies in confocal microscopy and performed a study examining the subcellular localization of the proteases during acute CVB3 infection of HeLa cells. It has been previously described that the poliovirus $3C^{pro}$ precursor 3CD, when expressed as a fusion protein, translocates into the nucleus after poliovirus infection or transfection with $2A^{pro}$, in a $2A^{pro}$ dependent manner (Sharma et al., 2004; Tian et al., 2011). Similarly, HRV16 3CD nuclear translocation is dependent on $2A^{pro}$ activity (Walker et al., 2016). Interestingly, according to our confocal microscopy results, both proteases appeared in the CVB3 infected HeLa cells within four hours after infection (Figures 4 and 5), and this timing of protease appearance was also supported by our Western blot data (Figure 1 C). The proteases mainly reside in the cell cytosol with an even distribution, whereas their nuclear localization was only faint or non-existent within the time frame of the studies (up to 6h post infection), suggesting that $2A^{pro}$ does not initiate similar protease translocation after CVB3 infection in our cell system.

On a final note, this study assessed the suitability of the newly developed 2A and 3C protease antibodies for use in various applications for the detection of proteases expressed in acute infection models. In future studies, it would be relevant to also assess if the antibodies are capable of detecting persistent EV infections, which have been shown to develop in the human heart muscle (Gaaloul et al., 2014; Luo et al., 2010). If the proteases were also expressed during persistent infections, this would suggest that the proteases might contribute to cell and tissue damage sustained during situations of viral persistence.

In conclusion, we describe three new antibodies that can detect the EV-B species proteases $2A^{pro}$ and $3C^{pro}$ and present a number of applications, in which they can be used. The antibodies described allow for the cross-validation of other methods and antibodies used to detect acute EV infections. Furthermore, the antibodies are suitable for use in studies examining the kinetics of infection, the subcellular localization of the proteases and may also be used to identify novel mechanisms by which the proteases contribute to tissue pathology. Such information can be used for the development of new antiviral therapies aimed at blocking virus replication and preventing tissue damage.

ACKNOWLEDGEMENTS

The authors wish to thank Rolle Rahikainen for his help in analyzing the confocal microscopy results. We also thank Jutta Laiho and Dr. Maarit Oikarinen for providing the cell microarray for the immunocytochemistry analyses. We would like to acknowledge the Karolinska Institutet including the Strategic Research Program in Diabetes, Sweden, the Swedish Child Diabetes Foundation and the Novo Nordic Foundation for financial support. OHL was supported by Vinnova, Sweden (diary number 2013-01330).

Declaration of Interest: HH is a minor (5%) shareholder and member of the board of Vactech Ltd, which develops vaccines against picornaviruses. The other authors have no conflict of interest to declare.

AUTHOR CONTRIBUTIONS

MFT and OHL designed the study with assistance from PGL and VPH. OHL planned antigen constructs together with VPH, did phylogenetic analyses and contributed to the antibody production and analysis of the results. PGL did cell microarray analyses. ES and ED participated to the initial screening of the clones and ES and ED together with VMS and PGL performed IHC of mouse tissue. VPH and JAEM contributed to antigen expression and purification. HH provided cell microarrays. SK performed Western blot. ES performed flow cytometry. MMH did the confocal microscopy. OHL and MFT wrote the manuscript and all other authors edited it and accepted the final form.

FIGURE LEGENDS

Figure 1. 2A-1 and 3C antibodies detect CVB proteases by Western blot.

(A,B) HeLa cells were infected with CVB3 (MOI 20). After 6 hours, infected cells were lysed and the proteases were detected by SDS-PAGE **(15 µg of cell lysate in each well)** and Western blot using the 2A-1 (A) and 3C (B) antibodies. Purified, recombinant $2A^{pro}$ and $3C^{pro}$ **(1 µg)** were used as positive controls. The band with an approximate size of ~50 kDa likely represents $3C^{pro}$ dimers (B). (C) HeLa cells were infected with CVB3 (MOI 20) and cultured for the indicated time periods, followed lysis and analysis by

SDS-PAGE **(15 µg of cell lysate)** and Western blot using the 2A-1 and 3C antibodies. D) HeLa cells infected with CVB1-6 (MOI 20) were lysed six hours post infection and proteases as well as VP1 were detected by SDS-PAGE **(15 µg of cell lysate)** and Western blot using antibodies 2A-I, 3C and VP1 antibody clone 5-D8/1. Beta actin was used as loading control (A-D).

Figure 2. $2A^{pro}$ and $3C^{pro}$ antibodies detect CVBs in murine tissue.

NOD (panels A-C and E-H) or C57BL/6J (panel D) mice were infected with CVB3 (B, D) or CVB5 (F, H) for 5 and 3 days, respectively. Uninfected control mice (A, C, E, and G) received buffer alone or remained untreated. Pancreases were removed, formalin fixed, sectioned and subjected to immunohistochemical staining using antibodies 2A-2, 3C or VP1 antibody 5-D8/1, as described in the materials and methods. E and G, and F and H, are consecutive tissue sections from the same tissue blocks. On representative tissue section per condition is shown, n = 1 - 2 mice per condition. The image magnification is 10X for A, B, 5X for C, D and 40X for E-H.

Figure 3. $2A^{pro}$ and $3C^{pro}$ antibodies identify infected cells by intracellular staining and flow cytometry. HeLa cells were infected with CVB3 (MOI 20) for 6h, after which they were fixed and permeabilized prior to intracellular staining with primary $2A^{pro}$ or $3C^{pro}$ antibodies. Primary antibodies were detected using a Phycoerythrin (PE) labeled secondary antibody ($2A^{pro}$ and $3C^{pro}$) and goat anti-mouse Alexa Fluor 647- (A) or Alexa Fluor 488-conjugated (B-C) secondary antibodies (VP1). Infection was confirmed by VP1 staining. One representative experiment out of n = 1 - 3 per condition is shown.

Figure 4. Confocal microscopy shows a time dependent appearance of $2A^{pro}$ and $3C^{pro}$ in the cytosol of CVB3 infected HeLa cells. HeLa-cells were infected with CVB3 (MOI 20) for 2, 4 and 6 h and stained for $2A^{pro}$ or $3C^{pro}$, nuclear lamin and nuclear DNA. A) CVB3 infected HeLa cells stained for nuclear DNA (DAPI; blue), nuclear lamina (red) and $2A^{pro}$ (green). B) HeLa cells infected with CVB3 stained for $2A^{pro}$ (black). C) Intensity profile of CVB3 infected HeLa-cells for lamin (red) and $2A^{pro}$ (green) antibodies at four hours post infection. This analysis was performed on the cell indicated by the white box in panel A. D) CVB3 infected HeLa-cells stained for nuclear DNA (DAPI; blue), nuclear lamina (red) and $3C^{pro}$ (green). E) HeLa-cells infected with CVB3 stained for $3C^{pro}$ (black). F) Intensity profile of CVB3 infected HeLa-cell for lamin (red) and $3C^{pro}$ (green) at six hour post infection. This analysis was performed on the cell indicated by white box in panel D. These figures are representative out of three separate experiments.

References

Badorff, C., Berkely, N., Mehrotra, S., Talhouk, J.W., Rhoads, R.E., Knowlton, K.U., 2000. Enteroviral protease 2A directly cleaves dystrophin and is inhibited by a dystrophin-based substrate analogue. J. Biol. Chem. 275, 11191–7.

Barnabei, M.S., Sjaastad, F. V, Townsend, D., Bedada, F.B., Metzger, J.M., 2015. Severe dystrophic cardiomyopathy caused by the enteroviral protease 2A-mediated C-terminal dystrophin cleavage fragment. Sci. Transl. Med. 7, 294ra106. https://doi.org/10.1126/scitranslmed.aaa4804

Calderaro, A., Arcangeletti, M.-C., Rodighiero, I., Buttrini, M., Gorrini, C., Motta, F.,

Germini, D., Medici, M.-C., Chezzi, C., De Conto, F., 2014. Matrix-assisted laser desorption/ionization time-of-flight (MALDI-TOF) mass spectrometry applied to virus identification. Sci. Rep. 4, 6803. https://doi.org/10.1038/srep06803

Calderón, K.I., Díaz-de Cerio, M., Otero, A., Muñoz-Almagro, C., Rabella, N., Martínez-Rienda, I., Moreno-Docón, A., Trallero, G., Cabrerizo, M., 2016. Molecular epidemiology of coxsackievirus B3 infection in Spain, 2004-2014. Arch. Virol. 161, 1365–70. https://doi.org/10.1007/s00705-016-2783-1

Ettischer-Schmid, N., Normann, A., Sauter, M., Kraft, L., Kalbacher, H., Kandolf, R., Flehmig, B., Klingel, K., 2016. A new monoclonal antibody (Cox mAB 31A2) detects VP1 protein of coxsackievirus B3 with high sensitivity and specificity. Virchows Arch. https://doi.org/10.1007/s00428-016-2008-8

Fairweather, D., Stafford, K.A., Sung, Y.K., 2012. Update on coxsackievirus B3 myocarditis. Curr. Opin. Rheumatol. 24, 401–7. https://doi.org/10.1097/BOR.0b013e328353372d

Feng, Q., Langereis, M.A., Lork, M., Nguyen, M., Hato, S. V, Lanke, K., Emdad, L., Bhoopathi, P., Fisher, P.B., Lloyd, R.E., van Kuppeveld, F.J.M., 2014. Enterovirus 2Apro targets MDA5 and MAVS in infected cells. J. Virol. 88, 3369–78. https://doi.org/10.1128/JVI.02712-13

Flodström, M., Maday, A., Balakrishna, D., Cleary, M.M., Yoshimura, A., Sarvetnick, N., 2002. Target cell defense prevents the development of diabetes after viral infection. Nat. Immunol. 3, 373–382. https://doi.org/10.1038/ni771

Gaaloul, I., Riabi, S., Harrath, R., Hunter, T., Hamda, K., Ghzala, A., Huber, S., Aouni, M., 2014. Coxsackievirus B detection in cases of myocarditis, myopericarditis, pericarditis and dilated cardiomyopathy in hospitalized patients. Mol. Med. Rep. https://doi.org/10.3892/mmr.2014.2578

Heikura, T., Nieminen, T., Roschier, M.M., Karvinen, H., Kaikkonen, M.U., Mähönen, A.J., Lesch, H.P., Rissanen, T.T., Laitinen, O.H., Airenne, K.J., Ylä-Herttuala, S., 2012. Baculovirus-mediated vascular endothelial growth factor-D(ΔNΔC) gene transfer induces angiogenesis in rabbit skeletal muscle. J. Gene Med. 14, 35–43. https://doi.org/10.1002/jgm.1637

Hühn, M.H., Hultcrantz, M., Lind, K., Ljunggren, H.-G., Malmberg, K.-J., Flodström-Tullberg, M., 2007. IFN-γ production dominates the early human natural killer cell response to Coxsackievirus infection. Cell. Microbiol. 0, 071027034427001–??? https://doi.org/10.1111/j.1462-5822.2007.01056.x

Jaïdane, H., Sané, F., Gharbi, J., Aouni, M., Romond, M.B., Hober, D., 2009. Coxsackievirus B4 and type 1 diabetes pathogenesis: contribution of animal models. Diabetes. Metab. Res. Rev. 25, 591–603. https://doi.org/10.1002/dmrr.995

Jaïdane, H., Sauter, P., Sane, F., Goffard, A., Gharbi, J., Hober, D., 2010. Enteroviruses and type 1 diabetes: towards a better understanding of the relationship. Rev. Med. Virol. 20, 265–280. https://doi.org/10.1002/rmv.647

Kramná, L., Kolářová, K., Oikarinen, S., Pursiheimo, J.-P., Ilonen, J., Simell, O., Knip, M., Veijola, R., Hyöty, H., Cinek, O., 2015. Gut virome sequencing in children with early islet autoimmunity. Diabetes Care 38, 930–3. https://doi.org/10.2337/dc14-2490

Laiho, J.E., Oikarinen, M., Richardson, S.J., Frisk, G., Nyalwidhe, J., Burch, T.C., Morris, M.A., Oikarinen, S., Pugliese, A., Dotta, F., Campbell-Thompson, M., Nadler, J., Morgan, N.G., Hyöty, H., JDRF nPOD-Virus Group, 2016. Relative sensitivity of immunohistochemistry, multiple reaction monitoring mass spectrometry, in situ hybridization and PCR to detect Coxsackievirus B1 in A549 cells. J. Clin. Virol. 77, 21–8. https://doi.org/10.1016/j.jcv.2016.01.015

Laiho, J.E., Oikarinen, S., Oikarinen, M., Larsson, P.G., Stone, V.M., Hober, D., Oberste, S., Flodström-Tullberg, M., Isola, J., Hyöty, H., 2015. Application of bioinformatics in probe design enables detection of enteroviruses on different taxonomic levels by advanced in situ hybridization technology. J. Clin. Virol. 69, 165–171. https://doi.org/10.1016/j.jcv.2015.06.085

Laitinen, O.H., Airenne, K.J., Hytönen, V.P., Peltomaa, E., Mähönen, A.J., Wirth, T., Lind, M.M., Mäkelä, K.A., Toivanen, P.I., Schenkwein, D., Heikura, T., Nordlund, H.R., Kulomaa, M.S., Ylä-Herttuala, S., 2005. A multipurpose vector system for the screening of libraries in bacteria, insect and mammalian cells and expression in vivo. Nucleic Acids Res. 33, e42. https://doi.org/10.1093/nar/gni042

Laitinen, O.H., Honkanen, H., Pakkanen, O., Oikarinen, S., Hankaniemi, M.M., Huhtala, H., Ruokoranta, T., Lecouturier, V., André, P., Harju, R., Virtanen, S.M., Lehtonen, J., Almond, J.W., Simell, T., Simell, O., Ilonen, J., Veijola, R., Knip, M., Hyöty, H., 2014. Coxsackievirus B1 is associated with induction of β-cell autoimmunity that portends type 1 diabetes. Diabetes 63, 446–55. https://doi.org/10.2337/db13-0619

Laitinen, O.H., Svedin, E., Kapell, S., Nurminen, A., Hytönen, V.P., Flodström-Tullberg, M., 2016. Enteroviral proteases: structure, host interactions and pathogenicity. Rev. Med. Virol. 26, 251–67. https://doi.org/10.1002/rmv.1883

Lamphear, B.J., Yan, R., Yang, F., Waters, D., Liebig, H.D., Klump, H., Kuechler, E., Skern, T., Rhoads, R.E., 1993. Mapping the cleavage site in protein synthesis initiation factor eIF-4 gamma of the 2A proteases from human Coxsackievirus and rhinovirus. J. Biol. Chem. 268, 19200–3.

Larsson, P.G., Lakshmikanth, T., Laitinen, O.H., Utorova, R., Jacobson, S., Oikarinen, M., Domsgen, E., Koivunen, M.R.L., Chaux, P., Devard, N.,

Lecouturier, V., Almond, J., Knip, M., Hyöty, H., Flodström-Tullberg, M., 2015. A preclinical study on the efficacy and safety of a new vaccine against Coxsackievirus B1 reveals no risk for accelerated diabetes development in mouse models. Diabetologia 58, 346–54. https://doi.org/10.1007/s00125-014-3436-0

Lei, X., Xiao, X., Xue, Q., Jin, Q., He, B., Wang, J., 2013. Cleavage of interferon regulatory factor 7 by enterovirus 71 3C suppresses cellular responses. J. Virol. 87, 1690–8. https://doi.org/10.1128/JVI.01855-12

Li, Y., Zhu, R., Qian, Y., Deng, J., Sun, Y., Liu, L., Wang, F., Zhao, L., 2011. Comparing Enterovirus 71 with Coxsackievirus A16 by analyzing nucleotide sequences and antigenicity of recombinant proteins of VP1s and VP4s. BMC Microbiol. 11, 246. https://doi.org/10.1186/1471-2180-11-246

Lim, B.-K., Peter, A.K., Xiong, D., Narezkina, A., Yung, A., Dalton, N.D., Hwang, K.-K., Yajima, T., Chen, J., Knowlton, K.U., 2013. Inhibition of Coxsackievirus-associated dystrophin cleavage prevents cardiomyopathy. J. Clin. Invest. 123, 5146–51. https://doi.org/10.1172/JCI66271

Lincez, P.J., Shanina, I., Horwitz, M.S., 2015. Reduced expression of the MDA5 Gene IFIH1 prevents autoimmune diabetes. Diabetes 64, 2184–93. https://doi.org/10.2337/db14-1223

Lind, K., Richardson, S.J., Leete, P., Morgan, N.G., Korsgren, O., Flodström-Tullberg, M., 2013. Induction of an antiviral state and attenuated coxsackievirus replication in type III interferon-treated primary human pancreatic islets. J. Virol. 87, 7646–54. https://doi.org/10.1128/JVI.03431-12

Lind, K., Svedin, E., Domsgen, E., Kapell, S., Laitinen, O., Moll, M., Flodström-Tullberg, M., 2016. Coxsackievirus counters the host innate immune response by blocking type III interferon expression. J. Gen. Virol. 97, 1–12.

https://doi.org/10.1099/jgv.0.000443

Lind, K., Svedin, E., Utorova, R., Stone, V.M., Flodström-Tullberg, M., 2014. Type III interferons are expressed by Coxsackievirus-infected human primary hepatocytes and regulate hepatocyte permissiveness to infection. Clin. Exp. Immunol. 177, 687–95. https://doi.org/10.1111/cei.12368

Luo, H., Wong, J., Wong, B., 2010. Protein degradation systems in viral myocarditis leading to dilated cardiomyopathy. Cardiovasc. Res. 85, 347–56. https://doi.org/10.1093/cvr/cvp225

Luoto, R., Jartti, T., Ruuskanen, O., Waris, M., Lehtonen, L., Heikkinen, T., 2016. Review of the clinical significance of respiratory virus infections in newborn infants. Acta Paediatr. 105, 1132–1139. https://doi.org/10.1111/apa.13519

Maccari, G., Genoni, A., Sansonno, S., Toniolo, A., 2016. Properties of Two Enterovirus Antibodies that are Utilized in Diabetes Research. Nat. Publ. Gr. https://doi.org/10.1038/srep24757

Man-Li, T., Szyporta, M., Fang, L.X., Kwang, J., 2012. Identification and characterization of a monoclonal antibody recognizing the linear epitope RVADVI on VP1 protein of enterovirus 71. J. Med. Virol. 84, 1620–7. https://doi.org/10.1002/jmv.23372

Massilamany, C., Gangaplara, A., Reddy, J., 2014. Intricacies of cardiac damage in coxsackievirus B3 infection: implications for therapy. Int. J. Cardiol. 177, 330–9. https://doi.org/10.1016/j.ijcard.2014.09.136

Miao, L.Y., Pierce, C., Gray-Johnson, J., DeLotell, J., Shaw, C., Chapman, N., Yeh, E., Schnurr, D., Huang, Y.T., 2009. Monoclonal antibodies to VP1 recognize a broad range of enteroviruses. J. Clin. Microbiol. https://doi.org/10.1128/JCM.00479-09

Mukherjee, A., Morosky, S.A., Delorme-Axford, E., Dybdahl-Sissoko, N., Oberste,

M.S., Wang, T., Coyne, C.B., 2011. The coxsackievirus B 3C protease cleaves MAVS and TRIF to attenuate host type I interferon and apoptotic signaling. PLoS Pathog. 7, e1001311. https://doi.org/10.1371/journal.ppat.1001311

N'Guyen, Y., Lesaffre, F., Metz, D., Tassan, S., Saade, Y., Boulagnon, C., Fornes, P., Renois, F., Andreoletti, L., 2016. Enterovirus but not Parvovirus B19 is associated with idiopathic dilated cardiomyopathy and endomyocardial CD3, CD68 or HLA-DR expression. Revised version R1. J. Med. Virol. https://doi.org/10.1002/jmv.24600

Oberste, M.S., Maher, K., Pallansch, M.A., 2004a. Evidence for frequent recombination within species human enterovirus B based on complete genomic sequences of all thirty-seven serotypes. J. Virol. 78, 855–67.

Oberste, M.S., Peñaranda, S., Pallansch, M.A., 2004b. RNA recombination plays a major role in genomic change during circulation of coxsackie B viruses. J. Virol. 78, 2948–55.

Oikarinen, S., Tauriainen, S., Hober, D., Lucas, B., Vazeou, A., Sioofy-Khojine, A., Bozas, E., Muir, P., Honkanen, H., Ilonen, J., Knip, M., Keskinen, P., Saha, M.-T., Huhtala, H., Stanway, G., Bartsocas, C., Ludvigsson, J., Taylor, K., Hyöty, H., VirDiab Study Group, 2014. Virus antibody survey in different European populations indicates risk association between coxsackievirus B1 and type 1 diabetes. Diabetes 63, 655–62. https://doi.org/10.2337/db13-0620

Orbach, R., Mandel, D., Lubetzky, R., Ovental, A., Haham, A., Halutz, O., Grisaru-Soen, G., 2016. Pulmonary hemorrhage due to Coxsackievirus B infection-A call to raise suspicion of this important complication as an end-stage of enterovirus sepsis in preterm twin neonates. J. Clin. Virol. 82, 41–5. https://doi.org/10.1016/j.jcv.2016.07.003

Persichino, J., Garrison, R., Krishnan, R., Sutjita, M., 2016. Effusive-constrictive

pericarditis, hepatitis, and pancreatitis in a patient with possible coxsackievirus B infection: a case report. BMC Infect. Dis. 16, 375. https://doi.org/10.1186/s12879-016-1752-3

Saarinen, N.V. V., Laiho, J.E., Richardson, S.J., Zeissler, M., Stone, V.M., Marjomäki, V., Kantoluoto, T., Horwitz, M.S., Sioofy-Khojine, A., Honkimaa, A., Hankaniemi, M.M., Flodström-Tullberg, M., Hyöty, H., Hytönen, V.P., Laitinen, O.H., 2018. A novel rat CVB1-VP1 monoclonal antibody 3A6 detects a broad range of enteroviruses. Sci. Rep. 8, 33. https://doi.org/10.1038/s41598-017-18495-4

Samuelson, A., Forsgren, M., Sällberg, M., 1995. Characterization of the recognition site and diagnostic potential of an enterovirus group-reactive monoclonal antibody. Clin. Diagn. Lab. Immunol. 2, 385–6.

Sharma, R., Raychaudhuri, S., Dasgupta, A., 2004. Nuclear entry of poliovirus protease-polymerase precursor 3CD: Implications for host cell transcription shut-off. Virology 320, 195–205. https://doi.org/10.1016/j.virol.2003.10.020

Tian, W., Cui, Z., Zhang, Z., Wei, H., Zhang, X., 2011. Poliovirus 2Apro induces the nucleic translocation of poliovirus 3CD and 3C??? proteins. Acta Biochim. Biophys. Sin. (Shanghai). https://doi.org/10.1093/abbs/gmq112

Walker, E., Jensen, L., Croft, S., Wei, K., Fulcher, A.J., Jans, D.A., Ghildyal, R., 2016. Rhinovirus 16 2A Protease Affects Nuclear Localization of 3CD during Infection. J. Virol. 90, 11032–11042. https://doi.org/10.1128/JVI.00974-16

Weidman, M.K., Yalamanchili, P., Ng, B., Tsai, W., Dasgupta, A., 2001. Poliovirus 3C protease-mediated degradation of transcriptional activator p53 requires a cellular activity. Virology 291, 260–71. https://doi.org/10.1006/viro.2001.1215

Wong, J., Zhang, J., Yanagawa, B., Luo, Z., Yang, X., Chang, J., McManus, B., Luo, H., 2012. Cleavage of serum response factor mediated by enteroviral protease

2A contributes to impaired cardiac function. Cell Res. 22, 360–71. https://doi.org/10.1038/cr.2011.114

Yagi, S., Schnurr, D., Lin, J., 1992. Spectrum of monoclonal antibodies to coxsackievirus B-3 includes type- and group-specific antibodies. J. Clin. Microbiol. 30, 2498–501.

Yeung, W.-C.G., Rawlinson, W.D., Craig, M.E., 2011. Enterovirus infection and type 1 diabetes mellitus: systematic review and meta-analysis of observational molecular studies. BMJ 342, d35.

Yousef, G.E., Brown, I.N., Mowbray, J.F., 1987. Derivation and biochemical characterization of an enterovirus group-specific monoclonal antibody. Intervirology 28, 163–70.

Zhang, A., Xiu, B., Zhang, H., Li, N., 2016. Protein microarray-mediated detection of antienterovirus antibodies in serum. J. Int. Med. Res. 44, 287–96. https://doi.org/10.1177/0300060515604981

Tables

Table 1. Detection of enteroviruses by the new $2A^{pro}$ and $3C^{pro}$ antibodies using immunocytochemistry and a comparison to the detection by the VP1 antibody clone 5-D8/1.

Cell line	Virus species	Serotype	2A-2[a]	3C[b]	VP1[c]
GMK	-	Uninfected	-	-	-
GMK	EV B	CVA9	+	+	+
GMK	EV B	CVB1	+	+	+
GMK	EV B	CVB2	+	+	+
GMK	EV B	CVB3	+	+	+
GMK	EV B	CVB4	+	+	+
GMK	EV B	CVB5	+	+	+
GMK	EV B	CVB6	+	+	+
GMK	EV B	Echo3	N/A	+	+
GMK	EV B	Echo4	+	+	+
GMK	EV B	Echo6	+	+	+
GMK	EV B	Echo9	-	+	+
GMK	EV B	Echo11	+	+	+
GMK	EV A	EV71	-	-	-
GMK	EV C	PV3	-	-	+
A549	-	Uninfected	-	-	-
A549	EV B	Echo30	+	+	+
A549	HPev	HPev1	-	-	-
RD	-	Uninfected	-	-	-
RD	EV A	CVA2	-	-	+
RD	EV A	CVA4	-	-	+
RD	EV A	CVA5	-	-	+

RD	EV A	CVA6	-	-	+
RD	EV B	CVA9	-	+	+
RD	EV A	CVA10	-	-	+
RD	EV A	CVA16	-	-	+
HeLa	-	Uninfected	-	-	-
HeLa	Adeno	Adeno C	-	-	-
Vero	-	Uninfected	-	-	-
Vero	EV A	CVA16	-	-	-

[a]Antigen retrieval: 10mM citrate, pH6

[b]Antigen retrieval: 10mM Tris 1mM EDTA, pH9

[c]Results from (Laiho et al., 2015)

N/A: Not Applicable

(+) indicates the presence of several brown cells within the sample

(-) indicates the absence of brown cells

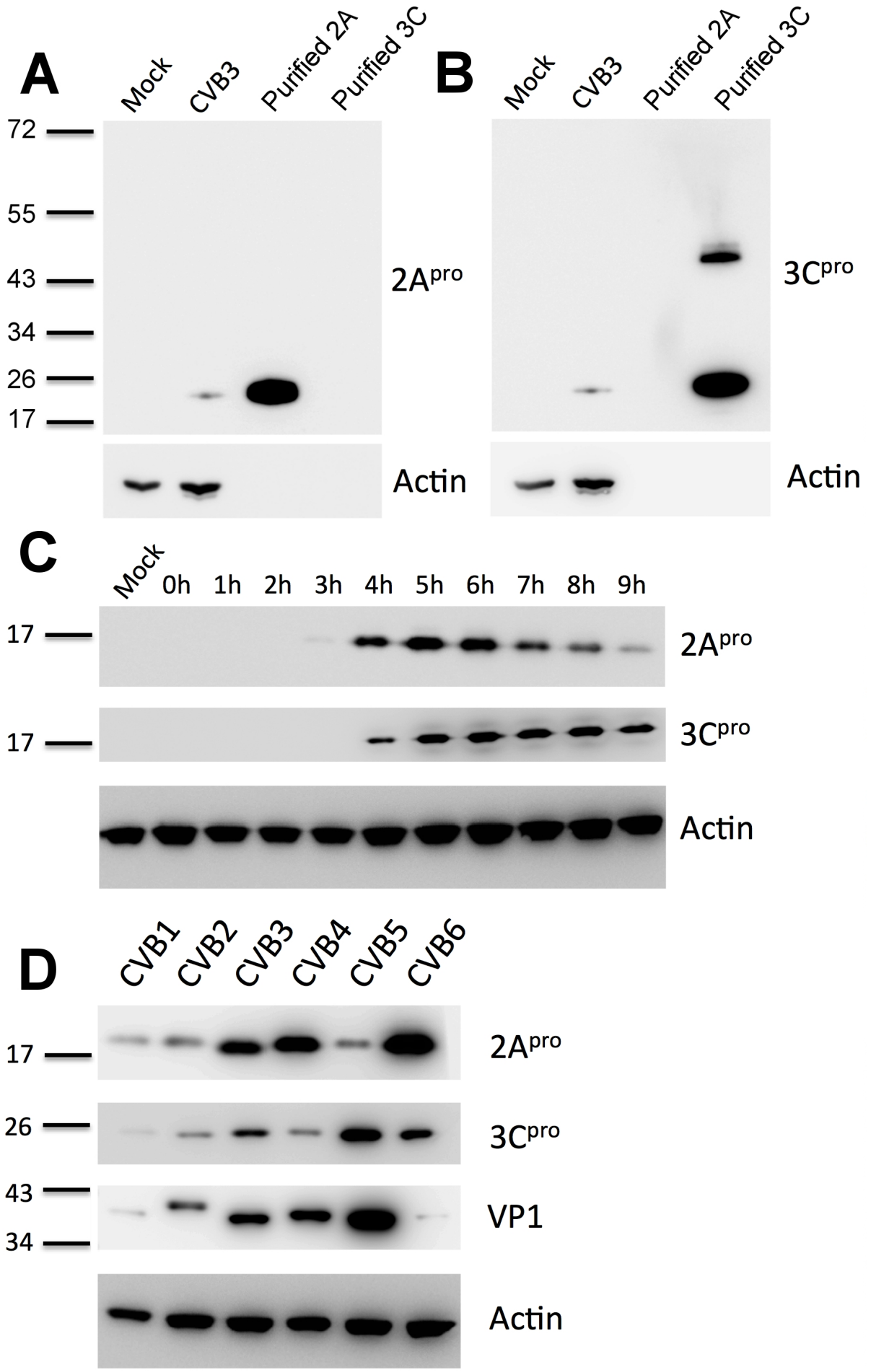
A
Mock
CVB3
Purified 2A
Purified 3C
72
55
43
34
26
17
2Apro
Actin
B
Mock
CVB3
Purified 2A
Purified 3C
3Cpro
Actin
C
Mock
0h
1h
2h
3h
4h
5h
6h
7h
8h
9h
17
2Apro
17
3Cpro
Actin
D
CVB1
CVB2
CVB3
CVB4
CVB5
CVB6
17
2Apro
26
3Cpro
43
34
VP1
Actin

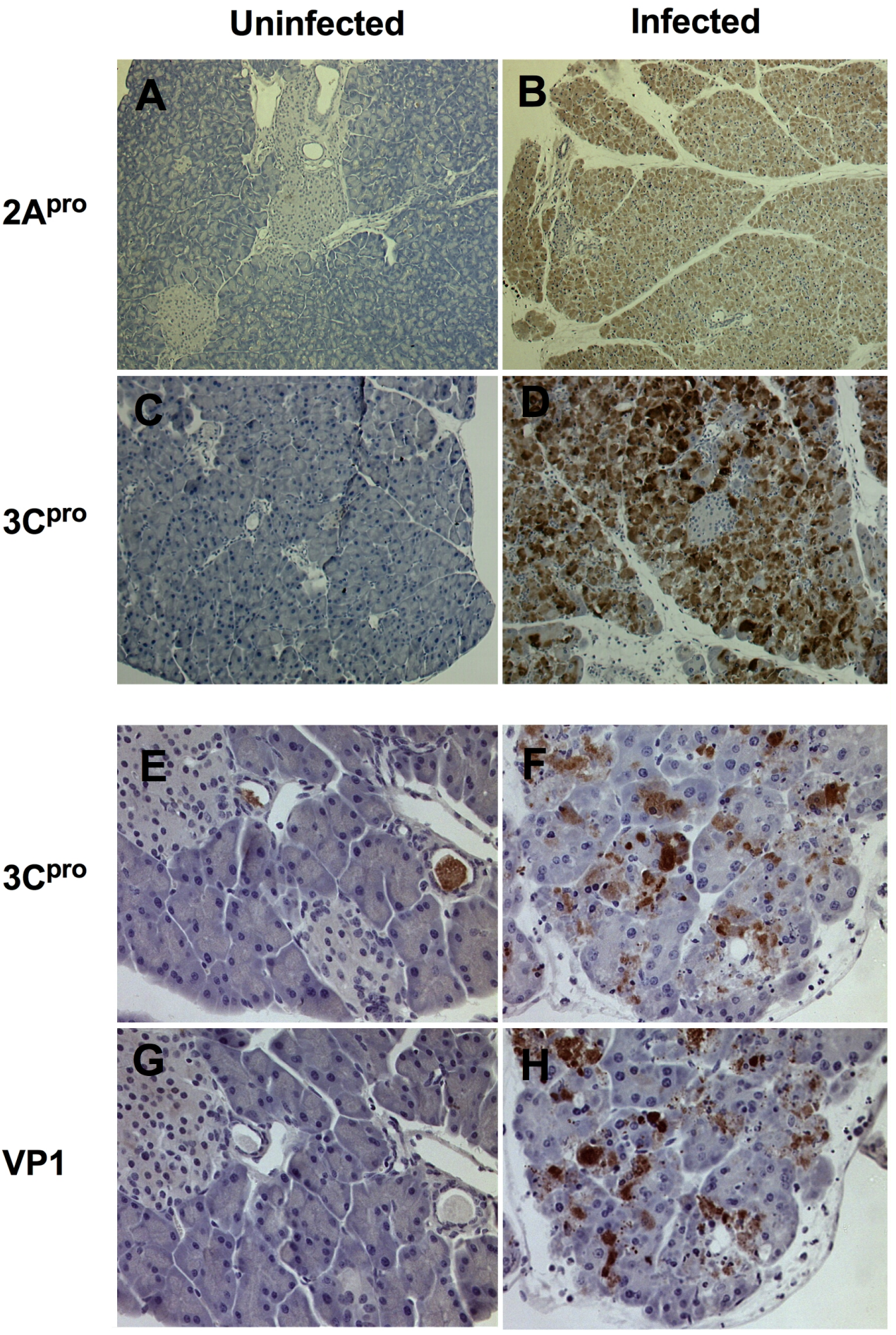
Uninfected
Infected
2A^pro
3C^pro
3C^pro
VP1
A
B
C
D
E
F
G
H

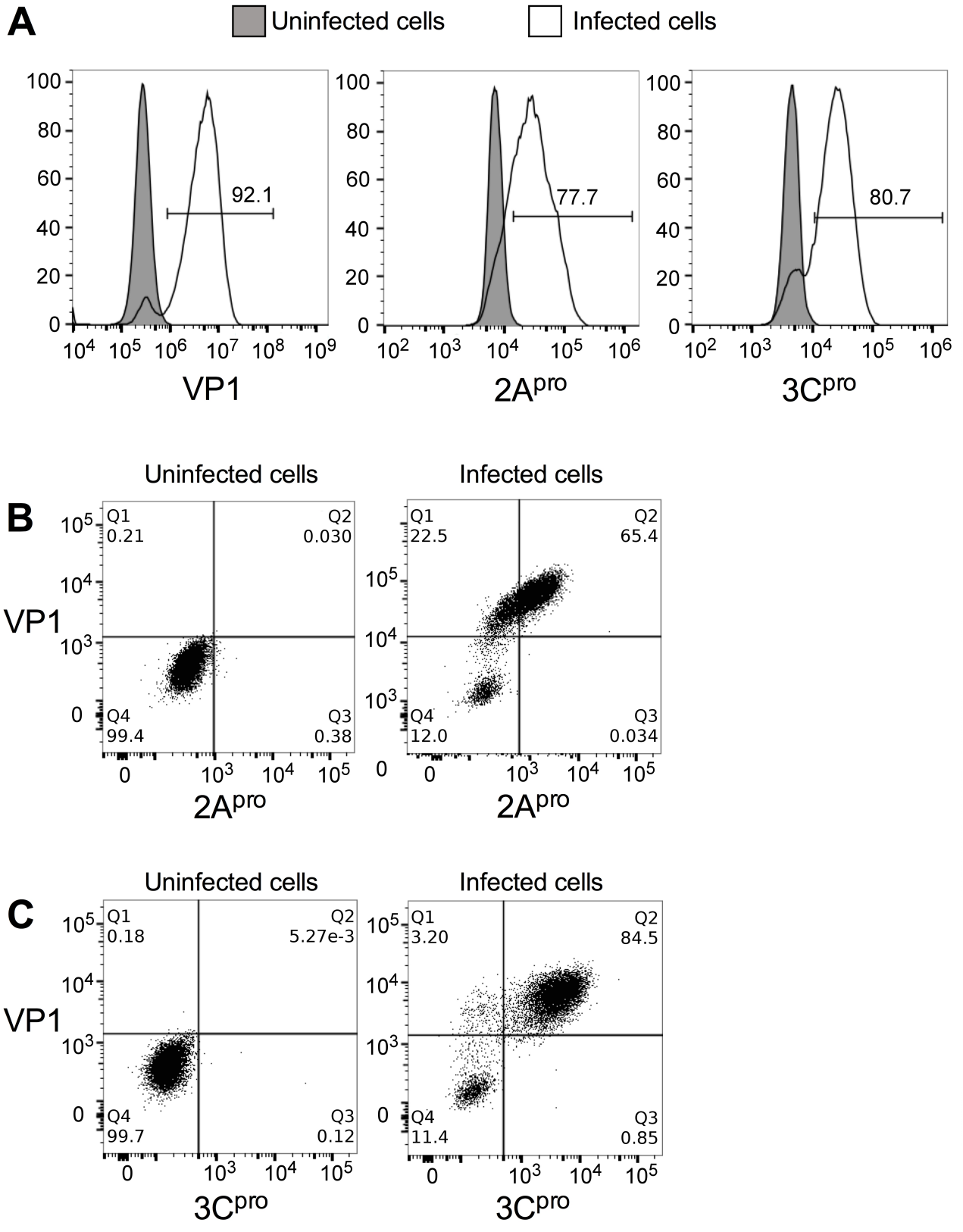
A
Uninfected cells
Infected cells
92.1
77.7
80.7
VP1
2Apro
3Cpro
B
Uninfected cells
Infected cells
Q1 0.21
Q2 0.030
Q4 99.4
Q3 0.38
Q1 22.5
Q2 65.4
Q4 12.0
Q3 0.034
VP1
2Apro
C
Uninfected cells
Infected cells
Q1 0.18
Q2 5.27e-3
Q4 99.7
Q3 0.12
Q1 3.20
Q2 84.5
Q4 11.4
Q3 0.85
VP1
3Cpro

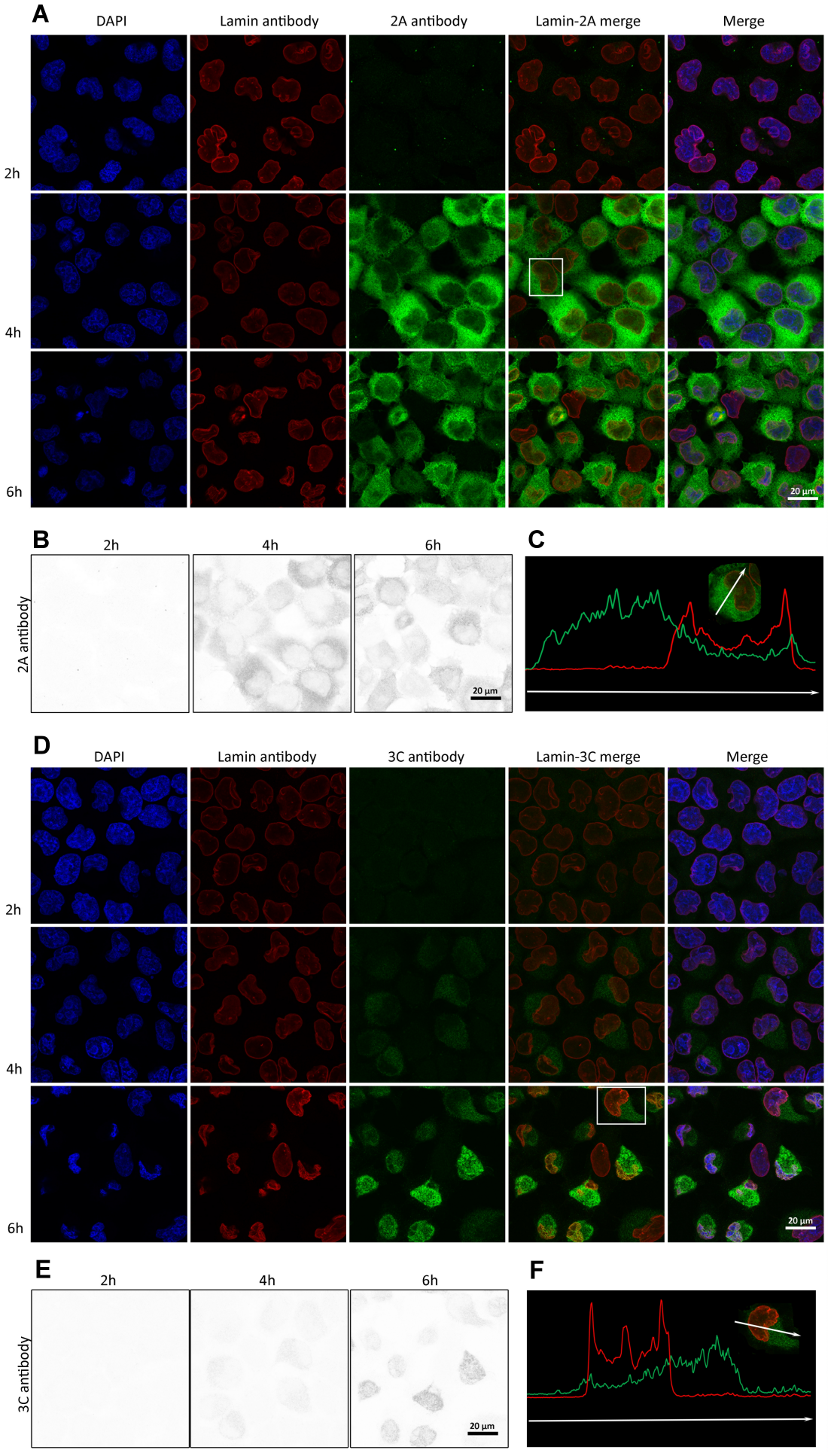
A
DAPI
Lamin antibody
2A antibody
Lamin-2A merge
Merge
2h
4h
6h
20 μm
B
2h
4h
6h
2A antibody
20 μm
C
D
DAPI
Lamin antibody
3C antibody
Lamin-3C merge
Merge
2h
4h
6h
20 μm
E
2h
4h
6h
3C antibody
20 μm
F

Electronic Supplemental Material for

New Coxsackievirus 2A^{pro} and 3C^{pro} protease antibodies for virus detection and discovery of pathogenic mechanisms

Olli H. Laitinen, Emma Svedin, Sebastian Kapell, Minna M. Hankaniemi, Pär G. Larsson, Erna Domsgen, Virginia M. Stone, Juha A. E. Määttä, Heikki Hyöty, Vesa P. Hytönen, Malin Flodström-Tullberg

Supplementary Materials and Methods

Phylogenetic analyses

Example sequences for each virus were fetched from the NCBI database and they were aligned with ClustalX (Larkin et al., 2007). The phylogenetic trees were generated with Mega 6 (Tamura et al., 2013). In each case, HPeV1 was manually set as the outgroup.

The detailed information about viruses used in the study

Supplementary table 1. Used viruses and their origin			
Virus species	**Serotype**	**Virus strain/origin**	**Used Methods**
EV B	CVA9	ATCC	CMA
EV B	CVB1	ATCC	CMA
	CVB1	CDC11 was isolated in Argentina at year 1998[1]	WB
EV B	CVB2	ATCC	CMA, WB
EV B	CVB3	ATCC Nancy	CMA, WB, IHC, FC, CM
EV B	CVB4	ATCC	CMA
	CVB4	E2[2]	WB
EV B	CVB5	ATCC	CMA, WB, IHC
EV B	CVB6	ATCC	CMA, WB
EV B	Echo3	PB-E3DiT23 isolated in Finland 1998[3]	CMA
EV B	Echo4	ATCC	CMA
EV B	Echo6	ATCC	CMA
EV B	Echo9	ATCC	CMA
EV B	Echo11	ATCC	CMA
EV A	EV71	PB-EV71Hus	CMA
EV C	PV3	Sabin	CMA
EV B	Echo30	ATCC	CMA
HPev	HPev1	ATCC Strain Harris	CMA
EV A	CVA2	PB-CVA2V38/Close resemblance to Coxsackievirus A2 isolate EV_NL_94 VP1 gene[4]	CMA
EV A	CVA4	PB-CVA4V36/Close resemblance to CVA4 isolate 10433, 2005 according to[5]	CMA
EV A	CVA5	PB-CVA5V43/ Close resemblance to isolate P-550/CA5/Kanagawa/2000[5]	CMA
EV A	CVA6	PB-CVA6V303V/Close resemblance to isolate CSF-1739/07 VP1[5]	CMA
EV B	CVA9	PB-CVA9V59/Close resemblance to FR-08-2005-149[5]	CMA
EV A	CVA10	PB-CVA10V2530/Close resemblance to P-2206/CA10/Kanagawa/2003[5]	CMA
EV A	CVA16	PB-CVA16V55/ Close resemblance to W42-44/01[5]	CMA
Adeno	Adeno C	VR 846	CMA
EV A	CVA16	ATCC	CMA

CMA, cell microarray; EV, enterovirus; CVA, Coxsackievirus A; CVB, Coxsackievirus B; IHC, immunohistochemistry; WB, Western Blot; FC, Flow cytometry; CM, Confocal microscopy
[1](Hämäläinen et al., 2014); [2](Kang et al., 1994); [3](Laiho et al., 2015); [4]Laitinen et al. unpublished; [5](Laitinen et al., 2014)

Supplementary results

Sequence alignments of proteases and VP1 support the antibody detection pattern observed with the experimental methods

In order to see how the proteases from the different viruses that were detected in the cell array by immunocytochemistry cluster, an example protein sequence for $2A^{pro}$, $3C^{pro}$ and VP1 were aligned and phylogenetic trees were generated for both proteases and VP1 separately (Supplementary Figures 1-3). This analysis indicated that virus strains are phylogenetically clustered at the antibody recognition patterns, further supporting the idea of epitope variation between virus species.

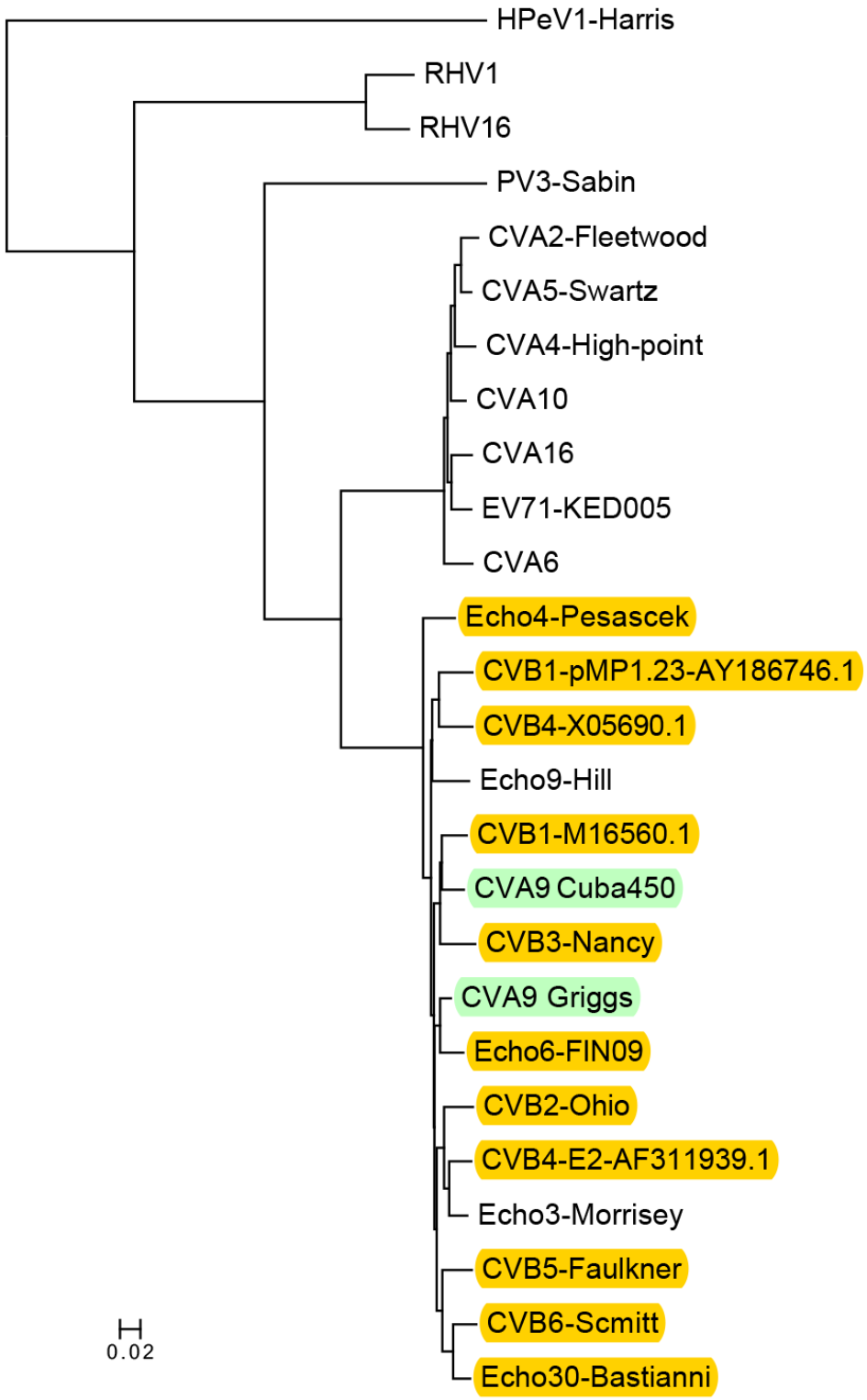

Supplementary Figure 1. Phylogenetic analysis of the 2A^{pro} part of the viruses used in the study. Viral proteases recognized by the 2A-2 antibody in immunocytochemical analysis are highlighted with orange color. The CVA9 2A^{pro} recognized in infected GMK cells but not in RD cells is marked with light green.

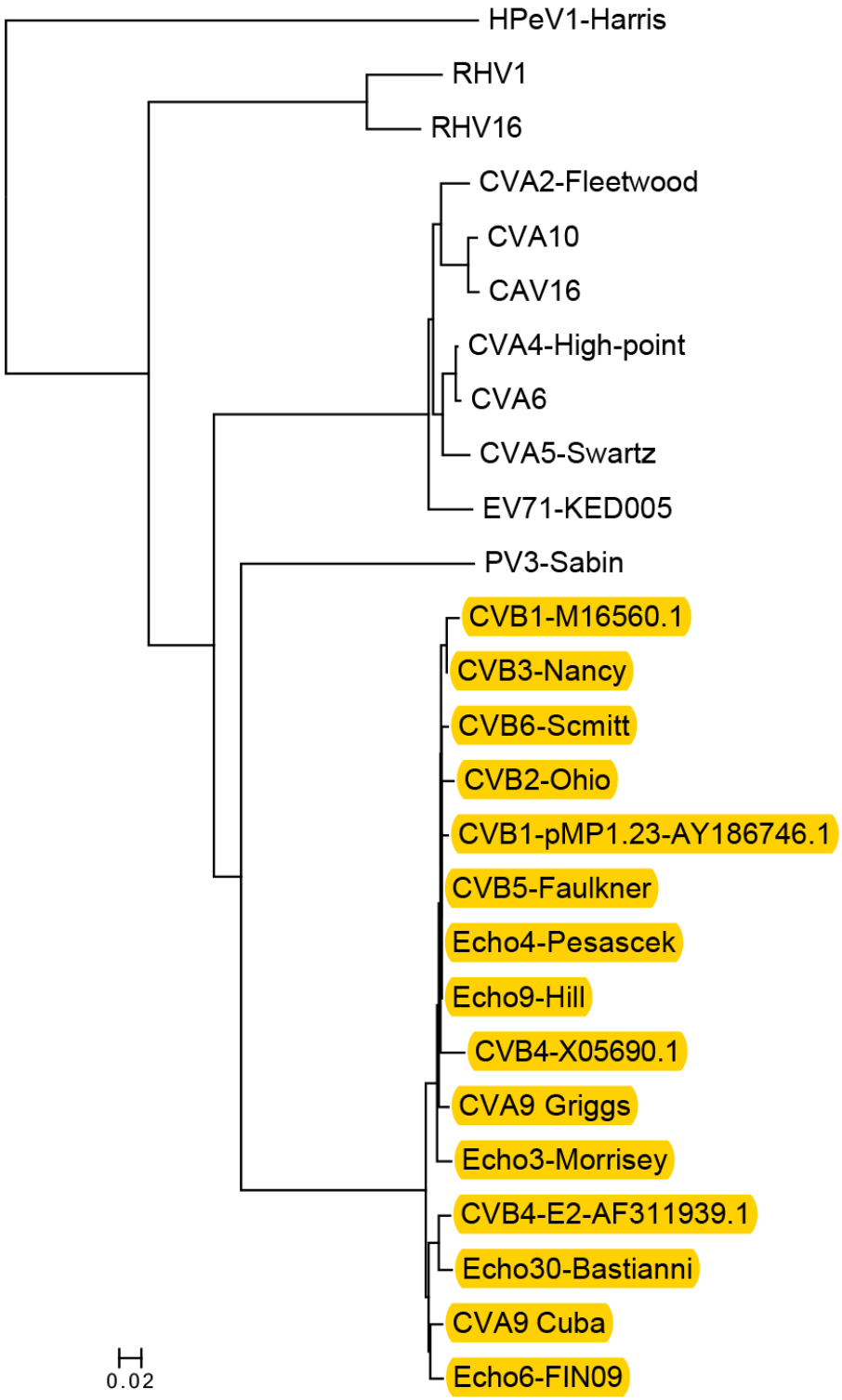

Supplementary Figure 2. Phylogenetic analysis of the 3C^{pro} part of the viruses used in the study. Viral proteases recognized by the 3C antibody in immunocytochemical analysis are highlighted with orange.

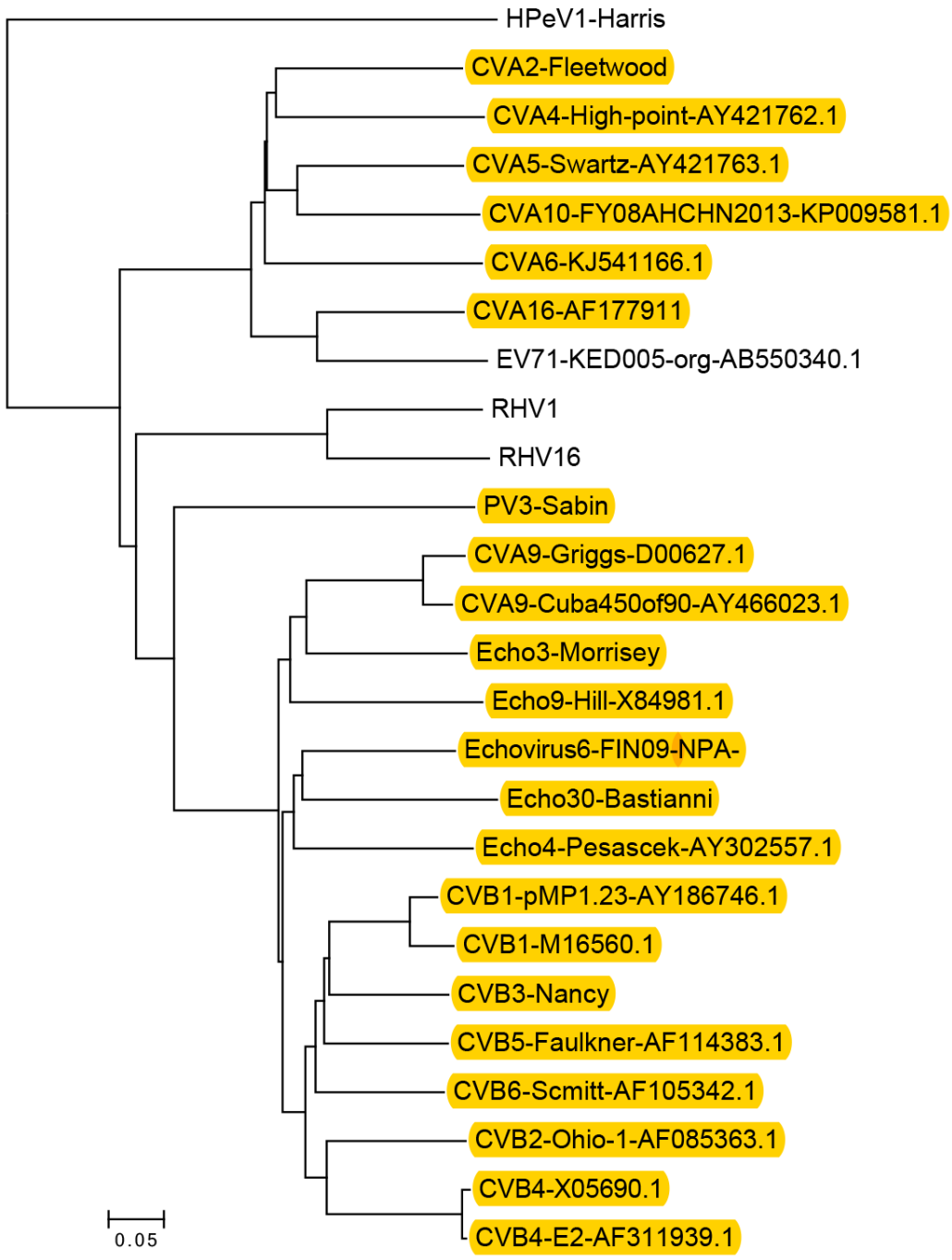

Supplementary Figure 3. Phylogenetic analysis of the VP1 part of the viruses used in the study. Viral proteases recognized by the anti-VP1 clone 5-D8/1 antibody in immunocytochemical analysis are highlighted with orange color.

Supplementary References

Hämäläinen, S., Nurminen, N., Ahlfors, H., Oikarinen, S., Sioofy-Khojine, A.-B., Frisk, G., Oberste, M.S., Lahesmaa, R., Pesu, M., Hyöty, H., 2014. Coxsackievirus B1 reveals strain specific differences in plasmacytoid dendritic cell mediated immunogenicity. J. Med. Virol. 86, 1412–1420. https://doi.org/10.1002/jmv.23903

Kang, Y., Chatterjee, N.K., Nodwell, M.J., Yoon, J.W., 1994. Complete nucleotide sequence of a strain of coxsackie B4 virus of human origin that induces diabetes in mice and its comparison with nondiabetogenic coxsackie B4 JBV strain. J. Med. Virol. 44, 353–61.

Laiho, J.E., Oikarinen, S., Oikarinen, M., Larsson, P.G., Stone, V.M., Hober, D., Oberste, S., Flodström-Tullberg, M., Isola, J., Hyöty, H., 2015. Application of bioinformatics in probe design enables detection of enteroviruses on different taxonomic levels by advanced in situ hybridization technology. J. Clin. Virol. 69, 165–171. https://doi.org/10.1016/j.jcv.2015.06.085

Laitinen, O.H., Honkanen, H., Pakkanen, O., Oikarinen, S., Hankaniemi, M.M., Huhtala, H., Ruokoranta, T., Lecouturier, V., André, P., Harju, R., Virtanen, S.M., Lehtonen, J., Almond, J.W., Simell, T., Simell, O., Ilonen, J., Veijola, R., Knip, M., Hyöty, H., 2014. Coxsackievirus B1 is associated with induction of β-cell autoimmunity that portends type 1 diabetes. Diabetes 63, 446–55. https://doi.org/10.2337/db13-0619

Larkin, M.A., Blackshields, G., Brown, N.P., Chenna, R., McGettigan, P.A., McWilliam, H., Valentin, F., Wallace, I.M., Wilm, A., Lopez, R., Thompson, J.D., Gibson, T.J., Higgins, D.G., 2007. Clustal W and Clustal X version 2.0. Bioinformatics 23, 2947–8. https://doi.org/10.1093/bioinformatics/btm404

Tamura, K., Stecher, G., Peterson, D., Filipski, A., Kumar, S., 2013. MEGA6:

Molecular Evolutionary Genetics Analysis version 6.0. Mol. Biol. Evol. 30, 2725–9. https://doi.org/10.1093/molbev/mst197